A Reactive Fourth-Harmonic Filter Operating at 400-kW CW

HANS J. MOHR, MEMBER, IEEE

Abstract—**A reactive fourth-harmonic filter operating at a fundamental power level of 400-kW CW is described. The filter, used in the NASA Deep Space Instrumentation Facilities, operates in an *S*-band (WR-430) waveguide run and it effectively attenuates the fourth harmonic of the fundamental transmit frequency near 2.1 GHz by a minimum of 40 dB. The design approach including power handling capability considerations is presented. Also included are some details of mechanical construction, tuning procedures, and results achieved.**

I. Introduction

THE NASA Deep Space Instrumentation Facilities employ a number of different transmitter-receiver combinations for performing various functions. A description of these systems is given by Hartop and Bathker [1]. One of the 400-kW CW transmitters operates in the 2.10- to 2.12-GHz frequency range. The receiver for an accompanying *X*-band system operates in 8.40- to 8.50-GHz frequency range. Thus the potential for *S*-band fourth harmonic interference with the *X*-band receiver is present.

The *S*-band transmitter employs an absorptive harmonic filter which attenuates the 2nd through 5th harmonics. This filter provides a minimum of 40-dB attenuation in the 8.40- to 8.48-GHz fourth-harmonic frequency range. Testing at Goldstone, however, indicated that this level of fourth-harmonic attenuation was insufficient, as indicated by excessive noise levels in the *X*-band receiver during *S*-band transmitter operation.

To solve this problem, Varian in 1972, was contracted by the Jet Propulsion Laboratory to design and fabricate a filter which would provide an additional 40 dB of fourth-harmonic attenuation, thereby providing a total system fourth harmonic attenuation in excess of 80 dB. The important electrical and mechanical specifications established for the filter were as follows.

Passband frequency range	2.10 to 2.12 GHz.
Passband insertion loss	0.05 dB max.
Passband VSWR	1.05 : 1 max.
Passband power capacity	500-kW CW.
Stopband frequency range	8.40 to 8.48 GHz.
Stopband attenuation (all modes)	40 dB min.
Size	61 cm (24 in) long $\times$ 61 cm (24 in) high $\times$ 35.5 cm (14 in) wide max.
Cooling: (H_2O at 60°C max.)	11.4 l/min. (3 gpm) at 0.35 kgm/cm^2 (5 psi) max.
Waveguide pressure: (nitrogen)	0.02 kgm/cm^2 (0.3 psig).

Manuscript received May 16, 1977; revised September 14, 1977.
The author is with Varian Associates, Inc., Palo Alto, CA 94303.

II. Design Approach

An important consideration in the design of any waveguide harmonic filter is careful examination of the possible modes of propagation in the stopband frequency range. Fig. 1 shows a normalized mode chart for WR-430 (10.92 $\times$ 5.46 cm (4.30 $\times$ 2.15 in)) waveguide. The chart is normalized to the cutoff frequency of the TE_{10} dominant mode. Included are the fundamental, second, third, fourth, and fifth harmonic frequency ranges corresponding to the 2.10- to 2.12-GHz fundamental frequency range. The mode chart shows that WR-430 waveguide will support 29 possible modes of propagation in the fourth-harmonic frequency range. To design an effective filter one should first reduce the number of possible modes by restricting waveguide cross-section and then employ filtering geometries which will efficiently attenuate the remaining modes.

Since there was no requirement for the filter to be absorptive, the number of possible propagating modes can be very significantly reduced by reducing the waveguide cross-sectional dimensions. For example, if the waveguide height is reduced sufficiently all TE_{mn} and TM_{mn} modes having $n > 0$ will be rejected. This is accomplished by choosing the narrow dimension of the waveguide such that the TE_{01} mode cutoff is slightly higher then the stopband frequency range, say 8.50 GHz. This results in a waveguide height of 1.75 cm (0.69 in). The result of this choice is to eliminate 23 of the possible 29 propagating modes leaving only the TE_{10}, TE_{20}, TE_{30}, TE_{40}, TE_{50}, and TE_{60} modes. These 6 remaining modes can be further reduced to 4 by restricting the waveguide width (broad dimension) to 8.76 cm (3.45 in). Thus by choosing waveguide dimensions of 8.76 cm (3.45 in) $\times$ 1.75 cm (0.69 in) only 4 modes can exist in the stopband frequency range. The problem of designing a filter to suppress 4 possible modes of propagation is greatly simplified as compared to suppressing 29 possible modes. Further reduction of the broad dimension to further reduce the number of possible modes was considered unwise since the dominant mode

0018-9480/78/0500-0341$00.75

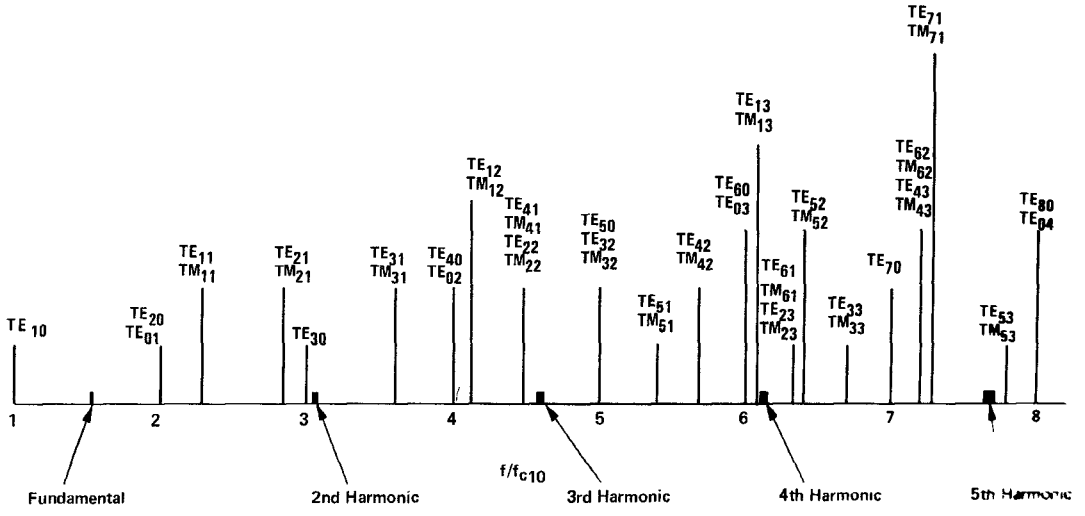

Fig. 1. Rectangular waveguide mode chart; 2:1 aspect ratio normalized to TE_{10} mode cutoff.

cutoff frequency would be moved too close to the operating frequency range. It is noted that the 8.76-cm broad dimension is approximately equal to the value for WR-340 waveguide which has a recommended lower operating frequency of 2.20 GHz. In view of the foregoing discussion, the problem has been reduced to designing a reactive fourth harmonic filter capable of rejecting TE_{10}, TE_{20}, TE_{30}, and TE_{40} modes.

The type of filter structure chosen utilized suitably spaced arrays of shorted stubs on the broadwalls. This type of filter, originally described by Rizzi [2], presented a means of achieving a reactive low-pass characteristic in a waveguide operating in the dominant mode. Rizzi's approach was extended to harmonic filters by Gerlack [3]. The basic approach is to provide arrays of shorted stubs on the broadwalls of the filter which are sensitive to all possible modes of propagation. A sketch of the filter geometry is shown in Fig. 2, which shows inclusion of metallic transverse septum plate along with the two broadwall stub arrays, thus providing two parallel waveguides having dimensions 1.75 cm (0.69 in) high by 8.76 cm (3.45 in) wide. Note that the stub arrays, dimensioned to react to the fourth-harmonic frequency range, are arranged in a 4 across pattern so as to be sensitive to the 4 possible modes of propagation.

Important considerations in the design of this type of filtering array are the transverse stub dimensions, the longitudinal stub spacing and the height of the stub array above the septum plate. Stub dimensions were chosen so that the stub cutoff frequency occurred just below the fourth-harmonic frequency range. Adequate metal was allowed between stubs to allow sufficiently large radii at the stub openings for insuring an adequate margin in power handling capability.

The longitudinal spacing of the stubs is normally chosen as a quarter guide wavelength at the reject band frequency. Because of mechanical spacing limits, however, $\lambda g/4$ spacing was not practical and a spacing of $3\lambda g/4$ was chosen, where λg is the average value for the TE_{10} mode and the TE_{20} mode at 8.4 GHz. It was reasoned that stubs tuned to reject the TE_{10} mode should also be effective for the TE_{30} mode. Similarly, stubs tuned to reject the TE_{20} mode should be effective for the TE_{40} mode.

The choice of spacing between the stub array and the septum plate was found empirically to be important in obtaining good filter performance. The originally chosen dimension was found to be unsuitable in that stub tuning was ineffective. By reducing the spacing sufficiently, effective coupling to the stub arrays was obtained and the final design incorporated 56 stub waveguides 10.1 cm (4 in) long arranged in a 4 across pattern on each broadwall.

III. Power Handling Capability

Perhaps the most important consideration in this filter design is that of power handling capability. The application required that the filter handle 500-kW CW. In addition to having adequate theoretical power handling capability, consideration must be given to geometrical configuration, operating temperature, waveguide atmosphere, altitude, and load VSWR. The theoretical waveguide breakdown power as given by Gould [4] can be calculated from

$$P = 1.33\,(10^{-3})ab(\lambda/\lambda_g)E_{\text{rms}}^2 \quad \text{W} \tag{1}$$

where $a = 8.76$ cm (3.45 in); $b = 1.75$ cm (0.69 in); $\lambda/\lambda_g = \sqrt{1-(\lambda/2a)^2} = 0.596$ at $f = 2.10$ GHz; and $E_{\text{rms}} = 29.000/\sqrt{2}$ V/cm for air at standard conditions. Therefore, the theoretical breakdown of the 8.76×1.75-cm filter waveguide is 5.11 MW.

An important power handling reduction factor is due to the radius at the stub opening. The final chosen radius r was 0.24 cm (0.093 in) while the width w of the opening was 0.79 cm (0.312 in). Referring to Cohn's [5] Fig. 11, the r/w value used here (0.298) results in an electric-field enhancement factor of 1.6, so that the power handling capability is reduced by 2.56.

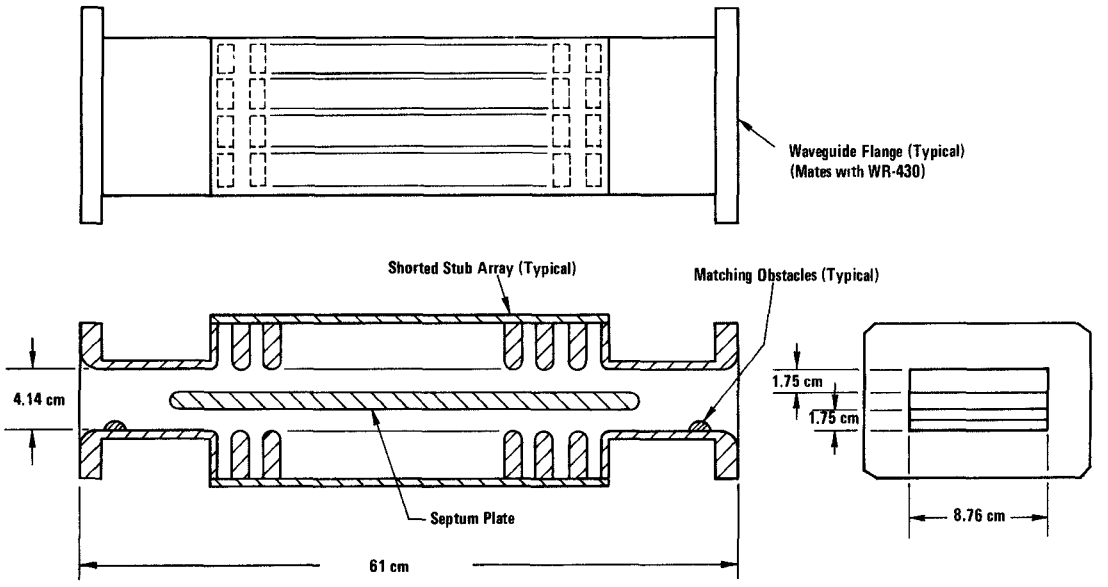

Fig. 2. Schematic layout—F430FA1 filter.

An additional conservative power reduction factor, used at Varian, to account for roughness on radii, has the empirically determined value of 1.7. The presence of nitrogen as waveguide gas contributes another power reduction factor of 1.7. A maximum load VSWR of 1.25 : 1 was assumed which yields a power reduction factor of 1.22. An altitude of 1000 m is assumed yielding a further power reduction factor of 1.18. Since the coolant temperature can reach 60°C, a final power reduction factor of 1.28 is required.

The net result of applying all of the above power reduction factors to the value of theoretical breakdown power calculated from (1) is that the 8.76-cm × 1.75-cm waveguide should breakdown at 375 kW. Since there are effectively two waveguides in parallel the filter will breakdown, under worst conditions, at 750 kW, yielding a 50-percent safety factor over the required 500-kW level.

An additional consideration is of importance in maintaining this safety margin in power handling capability. The radii at the ends of the septum plate must be sufficiently large so that breakdown will not occur due to electric field enhancement at the ends of the septum plate. Since the septum plate extends beyond the slotted portion on each end, as shown in Fig. 2, the slot reduction factor is not present. Thus it is only necessary to use a septum plate radius large enough so that the electric field enhancement factor does not exceed 1.6, the value due to the slots in the central portion of the filter. From Cohn's [5] Fig. 9, an electric field enhancement factor of 1.6 is obtained for $r/b = 0.35$. Since $b = 1.75$ cm, it follows that $r \geq 0.613$ cm.

IV. Mechanical Construction

The filter was fabricated entirely of OFHC copper and series 300 stainless steel. Hydrogen atmosphere furnace brazing techniques employing precious metal brazing alloys were used in fabrication, to insure clean flux-free braze joints. A first braze assembly consisted of assembly of the two broadwall stub arrays including mounting brackets. These stub arrays were joined to the side walls, flanges and septum plate in a second braze. A third braze was required to join the covers for the coolant channels and the passband matching obstacles. The coolant channels were designed to be integral with the filter narrow walls thus insuring efficient cooling of the filter body.

Following adjustment of the stub lengths to optimize the stopband rejection, cover plates were welded to the tops of the stub arrays, using tungsten inert arc welding techniques. This operation completes the pressure integrity of the unit. A photograph of the completed filter, designated model F430FA1, is shown in Fig. 3.

V. Tuning Procedures

Since standard WR-430 waveguide was mated abruptly, without transformer sections, to the 4.14 cm × 8.76 cm reduced cross section waveguide significant mismatches were introduced. The rather thick septum plate contributed further mismatches. An experimental program determined that the effects of both mismatches could be cancelled by using a single capacitive matching bar on each end of the filter. The matching obstacle can be seen in the sketch of Fig. 2 and in the photograph of Fig. 3.

A systematic tuning procedure was devised for optimizing the stopband performance of the filter. The design of the internal short circuits for tuning the stub lengths was such that each stub could be individually adjusted. The design incorporated a means of securely locking the short circuit in place following final adjustment.

In tuning the filter, attenuation as a function of frequency over the stopband frequency range was displayed on a network analyser oscilloscope. One half of the filter (one side of the septum plate) was terminated. Stopband energy was launched and detected in the TE_{10} mode and the 1st half of the stubs on the nonterminated

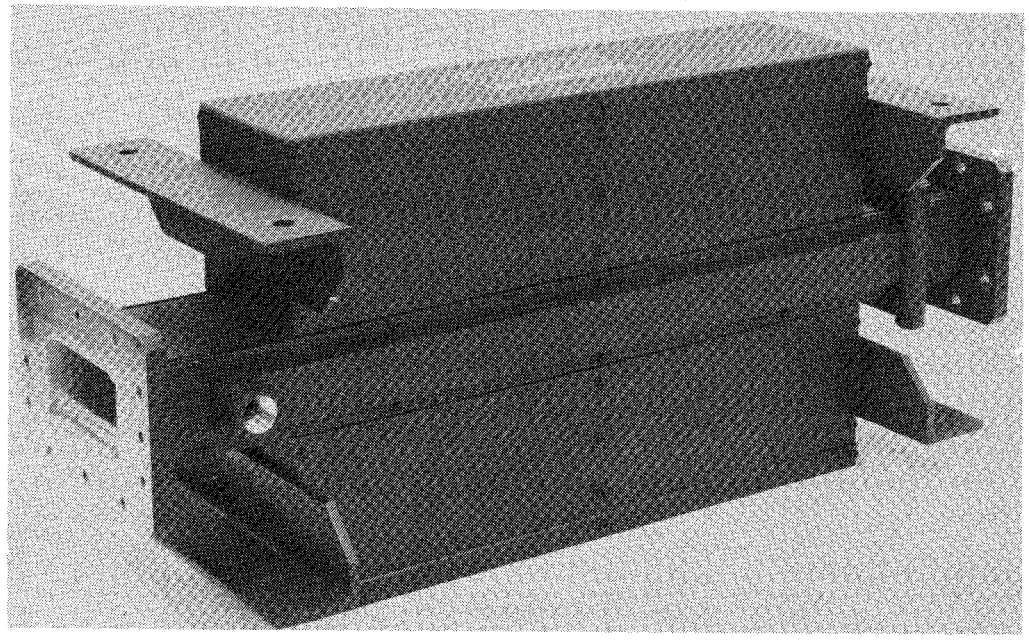

Fig. 3. Photograph of F430FA1 filter.

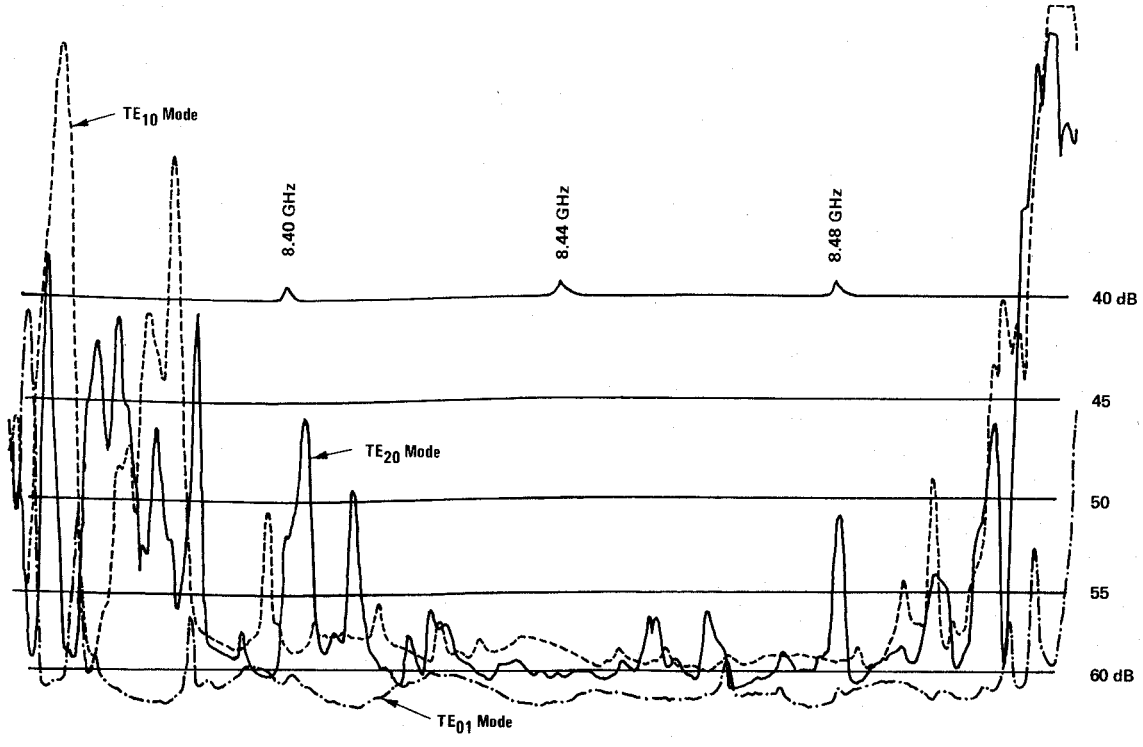

Fig. 4. F430FA1 filter; S/N 002 stopband attenuation.

side were adjusted for maximum attenuation. Next, energy was launched and detected in the TE_{20} mode and the remaining stubs were adjusted for maximum attenuation. The process was repeated for the other side of the filter by interchanging the termination. Finally the termination was removed entirely and some final trimming of stub lengths was done to optimize performance for the TE_{10} and TE_{20} modes. Following this procedure the individual short circuits were securely locked in place and the uniform cover plates were welded onto the top of the stub arrays.

VI. Results Achieved

A total of four filters was built and very similar performance was obtained on all units. Passband VSWR over the 2.10–2.12-GHz frequency range was less than 1.03 : 1 and passband insertion loss was less than 0.03 dB. As an example of the stopband attenuation achieved, data on one unit is presented in Fig. 4, which is a composite of swept frequency recordings of stopband attenuation for the TE_{10}, TE_{20}, and TE_{01} modes. TE_{01} mode stopband attenuation was measured (even though the mode cannot

exist in the filter) to insure that there was no conversion to any of the existing modes. Measurements in the TE_{30} and TE_{40} modes were not performed because of lack of suitable transitions for launching and detecting these modes.

The filters have been operated by NASA at passband power levels up to 400-kW CW without exhibiting arcing. Furthermore, the effectiveness of the filters has been demonstrated in that the improvements in X-band receiver noise levels is almost exactly the level indicated by the attenuation curves of Fig. 4 [6]. Thus a truly multimode fourth-harmonic filter operating at 400-kW CW has been demonstrated.

References

[1] R. Hartop and D. Bathker, "The high-power X-band planetary radar at Goldstone: Design, development, and early results," *IEEE Trans. Microwave Theory Tech.* vol. MTT-24, pp. 958–963, Dec. 1976.

[2] P. A. Rizzi, "Microwave filters utilizing the cutoff effect," *IRE Trans. Microwave Theory Tech.* vol. MTT-4, pp. 36–40., Jan. 1956.

[3] R. Z. Gerlack, "Waveguide reflective filter," U.S. Patent 3 611 214, Oct. 5. 1971.

[4] L. Gould, "Handbook of breakdown of air in waveguide systems," Microwave Associates, Inc., 22 Cummington St., Boston 15, MA, Navy Contract Nobsr63295, p. 7.

[5] S. B. Cohn, "Rounded corner in microwave high power filters and other components," *IRE Trans. Microwave Theory Tech.* vol. MTT-9, no. 5, pp. 389–397, Sept. 1961.

[6] R. L. Leu, JPL; Private communication.

X-Band High-Power Multipactor Receiver Protector

THOMAS P. CARLISLE

Abstract—**High vacuum devices incorporating the secondary electron resonance phenomenon have been used for several years in receiver protection circuits for high-power high-pulse repetition frequency (PRF) radars. These are known as multipactor devices. Recent technological developments have increased the peak-power handling capability and bandwidth of airborne-qualified devices to 50 kW and 12.5 percent, respectively. Life tests on multipactor devices have demonstrated 2500 h of failure free operation.**

I. Multipactor Phenomenon

A MULTIPACTOR DISCHARGE, or secondary electron resonance, is an electron phenomenon which can occur in a vacuum environment in the presence of microwave power. When the internal device dimensions and the RF voltages are such that electrons can be accelerated from one electrode to another in one half RF cycle, and the electrode surfaces have a secondary emission coefficient greater than unity, the density of electrons between the electrodes is multiplied.

An RF signal with electric field proportional to $\sin 2\pi ft$ applied across the gap between two electrodes can accelerate an electron in the gap to a velocity sufficient to cause δ secondary electrons to be emitted upon collision with one of the electrodes where δ is the coefficient of secondary emission of the electrode surfaces. If the amplitude of the electric field is such that the transit time across the gap is $1/(2f)$, i.e., one half RF cycle, and an initial electron is at one electrode at the beginning of an RF cycle, the electron will arrive at the other electrode and secondary electrons will be emitted at the same point in time as the RF voltage is changing sign. These secondary electrons are then accelerated back toward the original electrode. At the end of a full RF cycle, $1/f$, δ electrons arrive at the original electrode and δ^2 secondaries are emitted. This simple example leads to the result that the number of electrons in the gap increases by a factor of δ after each half RF cycle. The number of electrons in the gap is given by

$$N = N_0 \delta^{(2tf)} \tag{1}$$

where N equals the number of electrons at time t and N_0 equals the number of electrons at $t=0$ [1].

Electron multiplication according to (1) continues until space charge forces become sufficient to limit the density. The saturated electron volume density has been measured to be 3×10^{10} electrons/cm^3 [1]. Since the volume of a typical 10-GHz multipactor resonator is 10^{-2} cm^3 and if $\delta=5$ and $N_0=1$ are assumed, (1) shows that the multipactor discharge is fully saturated in 0.6 ns.

Once the electron discharge is established, a significant portion of the RF energy is converted into electron kinetic

Manuscript received May 13, 1977; revised August 23, 1977. This work was supported by the Air Force Materials Laboratory (LTE), Air Force Systems Command, Wright-Patterson AFB, Ohio under Air Force Contract F33615-74-C-5102.

The author is with Hughes Aircraft Company, Electron Dynamics Division, Torrance, CA 90509.

0018-9480/78/0500-0345$00.75